JHEP

Published for SISSA by Springer

Received: *September 10, 2016*
Revised: *October 20, 2016*
Accepted: *October 27, 2016*
Published: *November 11, 2016*

A Higgs in the warped bulk and LHC signals

F. Mahmoudi,[a,b,1] **U. Maitra,**[c] **N. Manglani**[d,e] **and K. Sridhar**[c]

[a] *Univ Lyon, Univ Lyon 1, ENS de Lyon, CNRS, Centre de Recherche Astrophysique de Lyon UMR5574, F-69230 Saint-Genis-Laval, France*

[b] *Theoretical Physics Department, CERN, CH-1211 Geneva 23, Switzerland*

[c] *Department of Theoretical Physics, Tata Institute of Fundamental Research, Homi Bhabha Road, Colaba, Mumbai 400 005, India*

[d] *Department of Physics, University of Mumbai, Kalina, Mumbai 400098, India*

[e] *Shah and Anchor Kutchhi Engineering College, Mumbai 400088, India*

E-mail: nazila@cern.ch, ushoshi@theory.tifr.res.in, namratam@physics.mu.ac.in, sridhar@theory.tifr.res.in

Abstract: Warped models with the Higgs in the bulk can generate light Kaluza-Klein (KK) Higgs modes consistent with the electroweak precision analysis. The first KK mode of the Higgs (h_1) could lie in the 1–2 TeV range in the models with a bulk custodial symmetry. We find that the h_1 is gaugephobic and decays dominantly into a $t\bar{t}$ pair. We also discuss the search strategy for h_1 decaying to $t\bar{t}$ at the Large Hadron Collider. We used substructure tools to suppress the large QCD background associated with this channel. We find that h_1 can be probed at the LHC run-2 with an integrated luminosity of 300 fb^{-1}.

Keywords: Beyond Standard Model, Field Theories in Higher Dimensions, Higgs Physics

ArXiv ePrint: 1608.07407

[1] Also Institut Universitaire de France, 103 boulevard Saint-Michel, 75005 Paris, France.

doi:10.1007/JHEP11(2016)075

JHEP11(2016)075

Contents

1 Introduction

The Randall-Sundrum model (RS model) [1], as originally proposed, is a five-dimensional model with a warped metric

$$ds^2 = e^{-2A(y)}\eta_{\mu\nu}dx^\mu dx^\nu - dy^2\,, \tag{1.1}$$

with the fifth dimension y compactified on an S^1/Z^2 orbifold of radius R. Two branes are located at $y = 0$ and $y = \pi R \equiv L$ and are called the UV and the IR branes respectively.

Starting with a bulk gravity action one can show that the solutions to the Einstein equation imply for the warp factor $A(y)$

$$A(y) = \pm k|y|\,, \tag{1.2}$$

where $k^2 \equiv -\Lambda/12M^3$ with M being the Planck scale. A value of $kL \sim 30$ is sufficient, through the warp factor, to generate a factor of $v/M \sim 10^{-16}$ (where v is the vacuum expectation value of the SM Higgs field) thereby stabilising the gauge hierarchy. This suppression factor is, however, material for all fields localised on the IR brane and, indeed, in the original RS model this was the case for all SM fields with only gravity localised in the bulk. With SM fields localised on the brane, mass scales which suppress dangerous higher-dimensional operators responsible for proton decay or neutrino masses also become small and this spells a disaster for the RS model.

Wisdom gleaned from AdS/CFT correspondence also gives an understanding of the need to go beyond the original RS model. The fields localised on the IR brane turn out, through the correspondence, to be composites of operators in the four-dimensional field theory that is dual to the RS model. The latter then turns out to be dual to a theory where all the SM fields are composite, which is not viable. However, a theory of partial compositeness is viable and can survive experimental constraints. This corresponds to a RS model where the SM fields are localised in the bulk.

This was, in fact, the motivation to move the SM fields into the bulk and construct what are called the Bulk RS models (for reviews, see refs. [2, 3]). In such models, often, the Higgs is still kept localised on the IR brane so that the gauge-hierarchy solution discussed above

JHEP11(2016)075

continues to hold. The big gain that accrues in the Bulk RS models is that the differential localisation of SM fermions in the bulk gives rise in a natural way to the Yukawa-coupling hierarchy [4–7]. The other features of Bulk RS models are that they give rise to small mixing angles in the Cabibbo-Kobayashi-Maskawa (CKM) matrix, provide a natural way of obtaining gauge-coupling universality and allow for the suppression of flavour-changing neutral currents [8–12].

As shown in later work on Bulk RS models,[1] even the Higgs need not be sharply localised on the IR brane but only somewhere close to it in order to address gauge-hierarchy. This freedom allows for more interesting model-building possibilities. It is this latter class of models which will be the focus of the present paper.

The serious issue to contend with in Bulk RS models is that of electroweak precision. In models with only gauge bosons propagating in the bulk, the constraints on the masses of the Kaluza-Klein (KK) gauge bosons are very strong (of the order of 25 TeV) [14–16] though this is somewhat ameliorated by also allowing SM fermions in the bulk, especially with fermions of the first and second generations localised close to the UV brane. Even in this case, there are unacceptably large couplings of the KK gauge bosons to the Higgs resulting in severe T-parameter constraints. One way of addressing this problem is called the Custodial symmetry model. In this model we have an enlarged gauge symmetry [17, 18] in the bulk, i.e an $\mathrm{SU}(3)_c \times \mathrm{SU}(2)_L \times \mathrm{SU}(2)_R \times \mathrm{U}(1)_y$ that acts like the custodial symmetry of the SM in protecting the ρ parameter and this extended group is then broken on the IR brane to recover the SM gauge group. This extended symmetry takes care of the T-parameter but non-oblique $Z \to b\bar{b}$ corrections, coming from the fact that the fermions are not all localised at the same point in the bulk, persist which are then addressed by a suitable choice of fermion transformations under the custodial symmetry group. The bound on the lightest KK gauge boson mode comes down to about 3 TeV [19, 20].[2]

The upshot of the above discussion is that, it is possible to get the masses of the KK modes of SM particles within the reach of collider searches. Indeed, there is already a significant amount of literature suggesting search strategies for KK gauge bosons [24–32] and KK fermions [33, 34] at the Large Hadron Collider (LHC). In contrast, KK modes of bulk Higgs have not received their due attention. The zero mode of the bulk Higgs has been studied in [35–37] and in [38] the CP-odd excitation of the bulk Higgs in the deformed metric model has been studied. It is to the search for the first KK excitation of the Higgs in the context of the custodial symmetric model at the LHC that we devote the rest of this paper.

2 Bulk Higgs models

The action with the Higgs propagating in the bulk [13] is given by

$$S = \int d^4x dy \sqrt{-g} (D_M \Phi D^M \Phi - m^2 \Phi^\dagger \Phi + 2 \sum_{j=0,1} (-1)^j \lambda^j(\Phi) \delta(y - y_j) + L_{\mathrm{yuk}}) \,, \qquad (2.1)$$

[1] For a review, see [13].

[2] There are other approaches in dealing with the electroweak precision constraints such as the deformed metric model [21, 22] or a model using brane kinetic term [23], but we will not consider these approaches here.

JHEP11(2016)075

where $y_0 = 0,\ y_1 = \pi R$,

$$\lambda^0 = \frac{M_0}{k}\Phi^\dagger\Phi\,, \quad -\lambda^1(\Phi) = -\frac{M_1}{k}|\Phi^\dagger\Phi| + 2\frac{\gamma}{k^2}|\Phi^\dagger\Phi|^2, \quad m^2 = ak^2$$

and

$$L_{\rm yuk} = y_5^{ij}\bar{\Psi}_i(x,y)\Psi_j(x,y)\Phi(x,y)\,.$$

λ^0 and λ^1 represent the scalar potentials on the UV and IR branes respectively. y_5 is the 5-dimensional Yukawa coupling. M_0 and M_1 are boundary mass terms on the UV and IR branes respectively. A quartic term is added on the IR brane to ensure electroweak symmetry breaking. a represents the dimensionless bulk mass parameter defined in the units of curvature, k.

Choosing

$$\Phi(x,y) = \frac{1}{\sqrt{2}}\begin{bmatrix} 0 \\ v(y) + H(x,y) \end{bmatrix}$$

and considering the metric given in eq. (1.1), the equation of motion for the vacuum expectation value (vev, $v(y)$) is given by (see appendix):

$$\partial_y(e^{-4ky}\partial^y v) + e^{-4ky}ak^2 v = 0\,,$$

with boundary conditions

$$(v\partial^y v)_{|\pi R} = \lambda^1(v(y=\pi R)) \ \text{ and } \ (v\partial^y v)_{|0} = 2\lambda^0(v(y=0))\,.$$

Similarly, the equation of motion for $H(x,y)$ is given by,

$$e^{-2ky}\partial_\mu\partial^\mu H(x,y) + e^{-4ky}ak^2 H(x,y) + \partial_y(e^{-4ky}\partial^y H(x,y)) = 0\,,$$

with boundary conditions

$$(H(x,y)\partial^y H(x,y))_{|\pi R} = \frac{\partial^2\lambda^1}{\partial H^2}_{|H=v} H^2 \ \text{ and } H(x,y)\partial^y H(x,y))_{|0} = \frac{\partial^2\lambda^0}{\partial H^2}_{|H=v} H^2\,.$$

$H(x,y)$ is a scalar field that can be expanded in terms of its KK tower as $f_n^h h_n/\sqrt{\pi R}$ where $h_n(x)$ is the nth KK field with mass m_n and $f_n^h(y)$ is the profile. The equation of the profile f_n^h is

$$-\partial_y(e^{-4ky}\partial_y f_n^h) + e^{-4ky}m^2 f_n^h = m_n^2 e^{-2ky} f_n^h\,, \tag{2.2}$$

where $\Box h_n = m_n^2 h_n$.

The profiles $f_n^h(y)$ satisfy the orthogonality relation given by

$$\int dy e^{-2ky} f_m^h f_n^h = \delta_{mn}\,. \tag{2.3}$$

The electroweak symmetry breaking occurs on the TeV brane and the zero mode (h_0 with $m_0 = 0$) gets its mass from the boundary potential on the TeV brane. Thus, the vev and the zero mode follow the same bulk profile and one can say that the vev of the Higgs field is entirely carried by the zero mode. The potential on the UV brane is chosen such

JHEP11(2016)075

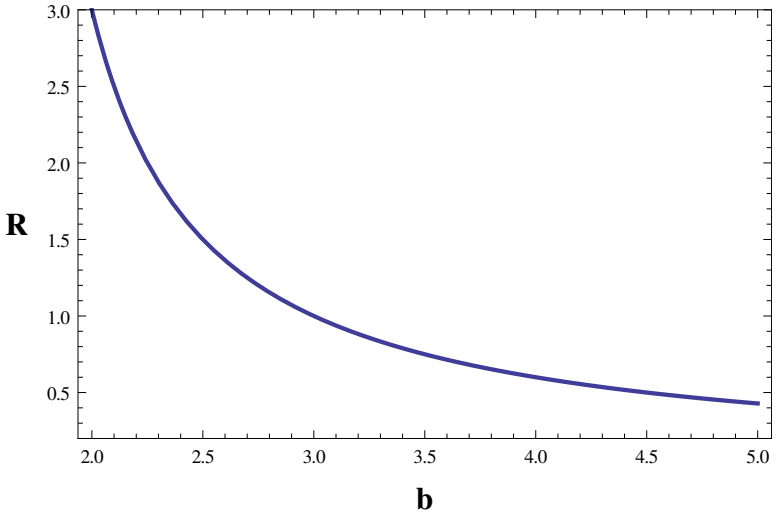

Figure 1. Variation of the ratio $R = M_{g_1}/M_{h_1}$ with b, where M_{g_1} is mass of the first KK mode of gluon.

that the profile of the zero mode and the vev localise on the TeV brane and the boundary condition on the TeV brane fixes the mass of the Higgs with the identification $M_1 = bk$. b represents the dimensionless brane mass parameter in units of k. Thus, we have

$$\Phi(x,y) = \frac{1}{\sqrt{2\pi R}} \begin{bmatrix} 0 \\ (v_{\rm SM} + h_0(x)) f_0^h(y) + h_n(x) f_n^h(y) \end{bmatrix},$$

where

$$f_0^h = \sqrt{\frac{(2(b-1)k\pi R)}{(e^{2(b-1)kR\pi} - 1)}} e^{(b-1)ky} \text{ and } b = 2 + \sqrt{4+a}\,.$$

Similarly, the bulk equation of motion of h_1 gives us the profile

$$f_1^h = 1.85\sqrt{kR\pi} e^{-k(R\pi - y)} \left(J_{b-2}\left(\frac{m_1 e^{ky}}{k}\right) + 0.36 Y_{b-2}\left(\frac{m_1 e^{ky}}{k}\right)\right),$$

having mass given by $m_1 = \left(1 + 2(b-2)\right)\frac{\pi}{4} k e^{-kR\pi}$.

From figure 1 we see that, depending on the value of b, the mass of h_1 can be as low as the third of the first gauge boson KK mode mass. This implies that the h_1 mass can be as low as a TeV in the custodial symmetry mode. When $b \gg 2$,[3] the mass of the h_1 is heavier and can not be directly probed at the LHC. In our analysis, we have considered a h_1 with mass of 1 TeV and beyond.

The gauge hierarchy problem gets solved by requiring that the zero KK mode of Higgs is close to IR brane. This implies that $b \geq 2$. In ref. [20], the precision electroweak analysis for models with the Higgs field in the bulk has been carried out in detail. In this analysis, three cases have been considered: 1) a model with a Higgs in the bulk without

[3]Note that b can not increase indefinitely as it implies a to be large. The product ak should be smaller than the 5-dimensional Planck mass. For $k/M_{\rm Pl} \sim 0.1$, the maximum allowed b is $\sim$ 5.

JHEP11(2016)075

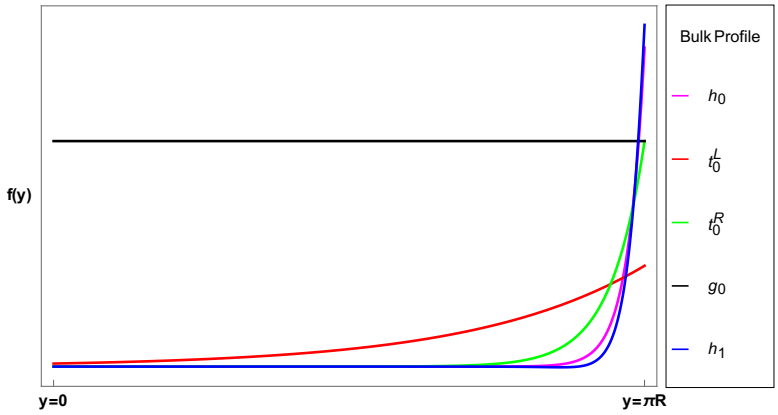

Figure 2. Profiles for the first KK mode of Higgs (blue), zero mode of Higgs (pink), zero mode of t^R (green), zero mode of t^L (red) and zero mode of gauge bosons (black).

any additional symmetry, 2) a bulk Higgs model enhanced with custodial $\mathrm{SU}(2)_L \times \mathrm{SU}(2)_R$ symmetry and 3) a model with a deformation of the metric near the IR brane. In each of these cases the oblique parameters at tree and loop levels and also the non-oblique constraints have been studied in tandem with the amount of fine-tuning required to get: a) the correct mass of the zero-mode Higgs scalar, and b) the correct solution to the gauge-hierarchy problem. The correlation between the infrared scale (Λ_{IR}) and the b parameter describing the bulk scalar then gives the best-fit points close to $b = 2$. For $b > 2$, the profiles tend to get exponentially peaked towards the IR brane and become more or less indistinguishable from a brane-localised Higgs. For our purposes, the region around $b = 2$ is the one that is of primary interest.

The profiles of the SM particles are plotted in figure 2. The couplings of the zero KK mode of Higgs (identified as the observed scalar at 125 GeV) to the SM particles are dictated by the profiles of the SM particles. As we have focused on $b = 2$, the zero KK mode of the Higgs is close to the IR brane. The profile of the zero mode of the gauge bosons are approximately flat ($\mathcal{O}(m_W/\Lambda_{\mathrm{IR}}) \ll 1$). Thus, there is a negligible deviation of the coupling of the zero KK mode of the Higgs to WW and ZZ from the SM Higgs coupling. The coupling of the Higgs to a pair of gluons are mediated by the loop of top quarks. In the loop along with the zero KK mode, the higher order KK modes of the top quark also contribute. The contribution of the loop can be approximated as $\mathcal{O}(y_5/\Lambda_{\mathrm{IR}})$ which is small as we have used $y_5 \sim 1$ in the following sections. For $y_5 \sim 1$, $\sigma^h_{ggF}/\sigma^{\mathrm{SM}}_{ggF}$ is within 5%. Similarly, the KK modes of fermions and SU(2) gauge bosons contribute in the loop of Higgs to diphoton and gives a deviation of about 5–7% [39]. These deviations are well within the uncertainty of the measured signal strength at the LHC [40–42].

The SM Higgs mixes with the radion, which is the field parameterizing the fluctuation between the two branes. In the limit of negligible back reaction, the kinetic term involving the radion and the Higgs induces the mixing [43]. As the vev of the bulk Higgs is carried out by the zero mode, the orthogonality condition prevents the mixing of the first KK mode with the radion.

JHEP11(2016)075

One can calculate the following tree-level interactions of the KK modes with the SM particles from the action (A.2),

- $h_1 \to V_0 V_0$: The term that governs the coupling is

$$\int d^4x dy h_1(x,y) W^+_\mu(x,y) W^{\mu-}(x,y)$$
$$= \int d^4x h_1(x) W^+_\mu(x) W^{\mu-}(x) g_5^2 \int dy \left(e^{(-2)ky} v_{\rm SM} f_0^h f_1^h \right). \tag{2.4}$$

  The zero KK mode of the gauge bosons (i.e the W_μ, Z_μ) have a flat profile[4] and thus, the tree level coupling vanishes following the orthogonality condition of the KK profiles given in (2.3).

- $h_1 \to h_0 h_0$: Unlike the radion-h_1 mixing term, this interaction comes from the quartic scalar potential added on the TeV brane (A.2) where the trilinear coupling of the SM Higgs is

$$\int dy d^4x \delta(y - R\pi)\sqrt{-g} \left(\frac{\partial^3 \lambda^1}{\partial H^3}_{|H=v} \right) \left(h_0 \frac{f_0^h}{\sqrt{\pi R}} \right)^3 \sim \int d^4x \lambda_{\rm SM} v_{\rm SM} h_0^3 \,, \tag{2.5}$$

  where $\lambda_{\rm SM} v_{\rm SM} = \dfrac{24\gamma v(y = R\pi)}{k^2} f_0^3(y = R\pi)$.
  The decay of the h_1 to SM Higgs is given by

$$\int dy d^4x \delta(y - R\pi)\sqrt{-g}\, 3 \left(\frac{\partial^3 \lambda^1}{\partial H^3}_{|H=v} \right) \left(h_0 \frac{f_0^h}{\sqrt{\pi R}} \right)^2 \frac{f_1^h}{\sqrt{\pi R}} h_1 \sim \int d^4x \lambda_{h1hh} v_{\rm SM} h_0^2 h_1 \,, \tag{2.6}$$

  where

$$\lambda_{h1hh} = 3 \frac{f_1}{f_0}_{|y=R\pi} \lambda_{\rm SM} \sim 3.2 \lambda_{\rm SM} \,. \tag{2.7}$$

  The δ-function has been integrated out.

- $h_1 \to t_0 t_0$: relative to the Yukawa coupling term of the SM Higgs to tops, where

$$y_5 \int dy d^4x \sqrt{-g} f_0^h f_0^{t^L} f_0^{t^R} h_0 t_0^L t_0^R \sim y_{\rm SM} \int d^4x h_0 t_0^L t_0^R \,, \tag{2.8}$$

  where $y_5 \int dy \sqrt{-g} f_0^h f_0^{t^L} f_0^{t^R} \sim y_{\rm SM}$, the decay of h_1 to tops is given by

$$y_{h1t^L t^R} = y_5 \int dy d^4x \sqrt{-g} f_1^h f_0^{t^L} f_0^{t^R} h_1 t_0^L t_0^R \,. \tag{2.9}$$

  Considering the reduced normalised profiles we can write the Yukawa coupling of h_1 to fermions with respect to the SM Yukawa coupling as follows:

$$y_{h1t^L t^R} = y_{\rm SM} \frac{\int dy f_1^h f_0^{t^L} f_0^{t^R}}{\int dy f_0^h f_0^{t^L} f_0^{t^R}} \,. \tag{2.10}$$

[4] In the limit $v/M_{kk} \ll 1$, the mixing between the KK mode of gauge bosons can be neglected and hence, the profile of the zero KK mode of the gauge bosons can be approximated flat.

JHEP11(2016)075

For a flat 5 metric, the reduced normalised profiles for zero-mode fermions is given by

$$f_0^{t_L} = \sqrt{\frac{(1-2c^L)\pi kR}{e^{(1-2c_L)\pi kR}-1}} e^{(\frac{1}{2}-c^L)ky}\,, \tag{2.11}$$

$$f_0^{t_R} = \sqrt{\frac{(1+2c^R)\pi kR}{e^{(1+2c^R)\pi kR}-1}} e^{(\frac{1}{2}+c^R)ky}\,. \tag{2.12}$$

Using the c^L=0.4 and c^R=0 and $b = 2$ we obtain

$$y_{h1t^Lt^R} = 1.0755\, y_{\rm SM}\,. \tag{2.13}$$

The partial decay widths of the KK Higgs to the pair of gluons, photons, tops and SM Higgs are given by,

$$\Gamma(h_1 \to gg) = (y_{h1t^Lt^R} y_{\rm SM})^2 \frac{M_{h_1}^3}{72\pi {v_{\rm SM}}^2} \left(\frac{\alpha_s}{\pi}\right)^2 \mid \Sigma_q I_q \mid^2,$$

$$\Gamma(h_1 \to \gamma\gamma) = (y_{h1t^Lt^R} y_{\rm SM})^2 \frac{M_{h_1}^3}{16\pi v_{\rm SM}^2} \left(\frac{\alpha}{\pi}\right)^2 \mid \Sigma_q I_q + \Sigma_l I_l \mid^2,$$

$$\Gamma(h_1 \to hh) = \lambda_{h1hh}^2 \frac{\lambda_{\rm SM}^2 {v_{\rm SM}}^2}{128\pi M_{h_1}} \sqrt{1-\frac{4m_h^2}{M_{h_1}^2}},$$

$$\Gamma(h_1 \to ff) = N_c (y_{h1t^Lt^R} y_{\rm SM})^2 \frac{m_f^2 M_{h_1}}{8\pi {v_{\rm SM}}^2} \left(1-\frac{4m_f^2}{M_{h_1}^2}\right)^{3/2}, \text{ where } N_c = 3.$$

In the above equations, $I_q = 3[2\lambda_q + \lambda_q(4\lambda_q - 1)f(\lambda_q)]$ and $I_l = 2\lambda_l + \lambda_l(4\lambda_l - 1)f(\lambda_l)$, where $\lambda_i = \dfrac{m_i^2}{M_{h_1}^2}$ are the form factors.

Having listed the couplings above for completeness, we would like to point out that the branching ratio of h_1 decaying to tops is overwhelmingly large as shown in figure 3. Thus, we focus on the $t\bar{t}$ decay mode of h_1 in this analysis.

The direct bounds on the electroweak observables coming from the h_1 in the loop will be suppressed as the coupling of h_1 to the SM gauge bosons vanish at the tree level. Thus, the only indirect constraint on the KK Higgs mass comes from the mass of the KK gauge boson. We assumed the mass of the first KK mode of gauge boson to be 3 TeV that puts a minimum constraint on the mass of h_1 to be 1 TeV for $b = 2$. The mass of the first KK mode of gluon is also considered at 3 TeV. The infrared scale is related to the mass of the 1st KK mode of gauge bosons as $m_1 = 0.75\pi\Lambda_{\rm IR}$. For mass of the KK gluon (M_{g_1}) at 3 TeV, our $\Lambda_{\rm IR}$ is 1.3 TeV.

Since, the couplings of the KK Higgs to the massive gauge bosons vanish at the tree level, the production of the KK Higgs via vector boson fusion is heavily suppressed. As the Yukawa coupling of the tops with the KK Higgs is of $\mathcal{O}(1)$, the KK Higgs can be produced in association with tops or via gluon-gluon fusion with tops running in the loop. The associated production of the KK Higgs with tops is suppressed by two orders of magnitude in this mass range. Thus, the only dominant production mode of the KK Higgs

JHEP11(2016)075

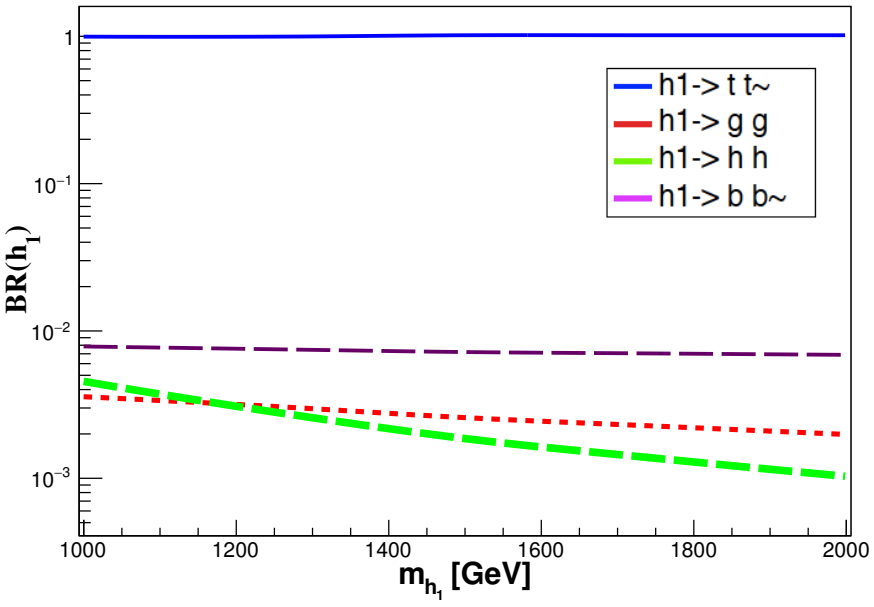

Figure 3. Branching ratio of the KK Higgs in $t\bar{t}$ (solid blue line), $b\bar{b}$ (dashed magenta line), gg (dashed red line) and hh (dashed green line) channels as a function of the KK Higgs mass.

is via gluon-gluon fusion. Even before we launch into our analysis, we should check what constraints existing collider data from $t\bar{t}$ production places on a 1 TeV resonance decay. Recently, the ATLAS [44] and the CMS [45] collaborations at the LHC have presented their measurements of the top cross-section at $\sqrt{s} = 13$ TeV. The values of the cross-section from both experiments are in agreement with NNLO QCD predictions of the cross-section. The CMS experiment, analysing 43 pb^{-1} of data, has quoted an error of the order of 86.5 pb on the cross-section and the ATLAS experiment, analysing a larger 3.2 fb^{-1} sample, has an error of the order of 36 pb. For a 1 TeV mass h_1, the cross-section is much smaller (of the order of 0.5 pb). Therefore, present measurements of the $t\bar{t}$ cross-section are not sensitive to the h_1.

3 h_1 at the LHC

As discussed earlier, the h_1 is produced via gluon-gluon fusion with tops propagating in the loop and it further decays to $t\bar{t}$ at the LHC. Thus, our signal is characterised by two tops. Model files have been obtained with `FEYNRULES` [46], and the signal events are generated by interfacing it with `MADGRAPH` [47] with the parton distribution function `NNLO1` [48]. Since, we are considering the scalar having mass beyond TeV, the tops coming from the scalar are in the boosted regime with most of the tops having transverse momentum in the range of 200–800 GeV as can be seen from figure 4 and the decay products of the top will mostly lie in a single hemisphere as can be seen in figure 5.

To optimise the signal, we have considered the hadronic decay of tops that can be tagged using the HEPTopTagger [49, 50] algorithm. The backgrounds for our signal can be categorised as

JHEP11(2016)075

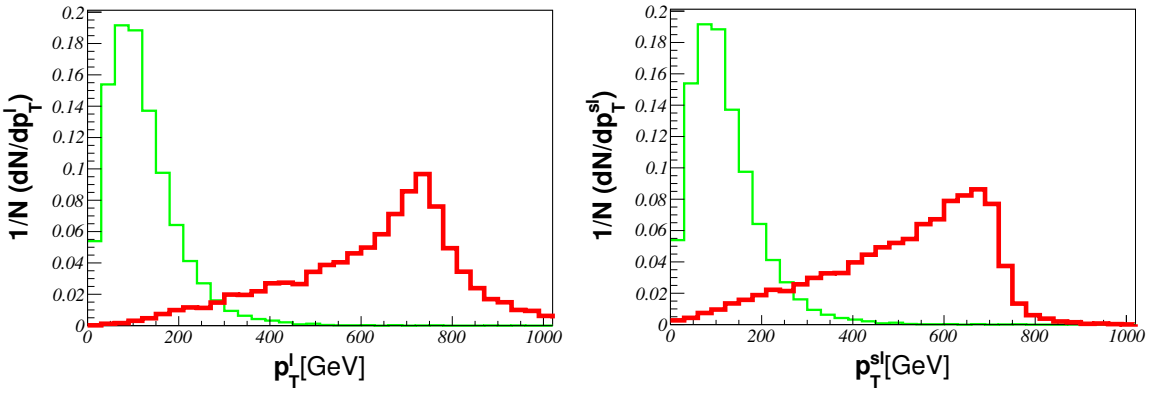

Figure 4. Normalised distribution of the p_T for leading top (left) and subleading top (right), for $M_{h_1} = 1.5\,\text{TeV}$. The red distribution represents signal and green represents $t\bar{t}$ background.

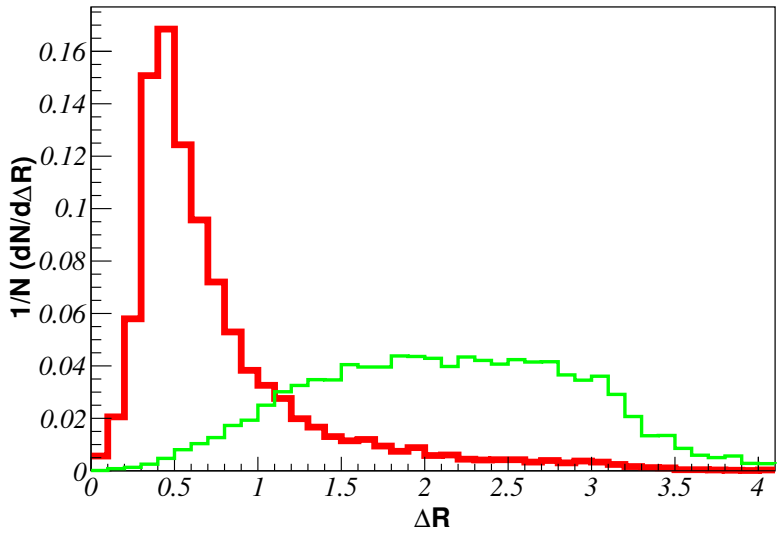

Figure 5. Normalised distribution of the angular separation between the decay products of the top, for $M_{h_1} = 1.5\,\text{TeV}$. The red distribution represents signal and green represents $t\bar{t}$ background.

- Reducible background: the dominant reducible background in this topology is the dijet background. Once we demand top tagging, this background reduces drastically. It can be controlled further using a high transverse momentum (p_T) cut on the tagged top.

- Irreducible background: the irreducible background arises from the pair production of tops via QCD processes. As expected, the tagging efficiencies of the two tops are similar to the signal and hence, we need to use the decay kinematics to isolate the signal.

The SM $t\bar{t}$ and dijet events are generated using `PYTHIA 8` [51]. The showering and the hadronisation of the signal event as well as the background events have been carried out using `PYTHIA 8`. To generate background events with larger statistics we have divided our

JHEP11(2016)075

analyses into different phase space regions[5] depending upon the mass of the KK Higgs that we are probing. In figure 4, we have plotted the distribution of transverse momentum at the parton-level for leading (sub-leading) tops from h_1 having a mass of 1.5 TeV and SM $t\bar{t}$ background. As discussed earlier, the transverse momenta of tops coming from h_1 are mostly peaked near half of the h_1 mass whereas the SM backgrounds largely peak at the lower transverse momentum region. Also, the decay product of the tops coming from the signal can be encompassed within a fat jet of radius ~ 1.5 (figure 5). Keeping this in mind, we split our analysis into two regions. In the first region, we have reconstructed the jets using the Cambridge Aachen (C-A) algorithm [52, 53] with jet radius (R = 1.5), $p_T > 250\,\text{GeV}$ and $|\eta| < 2.4$. In the second region we have used a slightly higher value of transverse momentum to reconstruct the fat jet i.e $p_T > 350\,\text{GeV}$. The first part is optimised for the search of the h_1 in the range of 1 TeV whereas the second region is proposed when its mass is around 1.5 TeV and beyond.

These two fat jets are then considered as an input for the HEPTopTagger. The algorithm of the HEPTopTagger is briefly described here,

- Un clustering: the fat jet (J) is split into subjets j_i using mass-drop criterion minimum $m_{j_i} < 0.8 m_J$. The subjets that satisfy $m_{j_i} < 30\,\text{GeV}$ are not considered.
- Filtering: the unclustered subjets are filtered with $R_{filt} = 0.3$ and the fat jets with three subjets which give a total jet mass close to the top mass are considered further.
- Kinematic Selection: the three subjets are then made to satisfy top decay kinematics. One can construct three pairs of invariant mass with these three subjets out of which two of them are independent. In the two dimensional space determined by the pair of invariant mass, top-like jets represent a thin triangular annulus (as one of them always reconstructs a W). On the other hand, the background is concentrated in the region of small pair-wise invariant mass.

We consider two such 'top-tagged' jets for our further analysis. At this stage, we have very few (almost negligible) events coming from the dijet background. The h_1 is produced mostly at rest: as a result the top pairs are back to back. We have plotted the distribution of the absolute value of difference in rapidity ($|\Delta\eta|$) of the 'top-tagged' pair coming from the signal as well as from the SM background in figure 6. For the $t\bar{t}$ background, the distribution peaks near $|\Delta\eta| \sim 0$ whereas the tops coming from the signal have a larger spread. We found that a minimum cut on $\Delta\eta$ helps us to isolate the signal from background. When the mass of the KK Higgs is around 1 TeV, we have selected events with transverse momentum of the 'top-tagged' pairs (p_T^l and p_T^{sl}) greater than 400 and 350 GeV respectively. The combination of the minimum cut on the transverse momentum and the minimum cut on pseudorapidity helps us to suppress the dijet background further. The efficiency of the minimum cut on $\Delta\eta$ increases as the mass of the KK Higgs increases. Thus, for the KK Higgs having a mass of 1.5 TeV and beyond, a minimum cut on pseudorapidity is sufficient to reduce QCD as well as $t\bar{t}$. After the angular cut, we made sure that the tops coming from the signal reconstruct the h_1 mass. We enhance the signal efficiency by demanding that the

[5] $\hat{p_T} > m_{h_1} - 600\,\text{GeV}$ and $\hat{m} \in (m_{h_1} - 300\,\text{GeV}, m_{h_1} + 300\,\text{GeV})$ where hat represents outgoing parton system.

JHEP11(2016)075

Mass (GeV)	Cuts	Signal (fb)	QCD (fb)	$t\bar{t}$ (fb)
1000	2 fat jets ($p_T > 250\,\text{GeV}$, $R < 1.5$)	52.36	395183.24	404.80
	2 top-tagged jets	2.64	65.11	27.04
	$p_T^l > 400\,\text{GeV}$ and $p_T^{sl} > 350\,\text{GeV}$	1.43	58.33	26.66
	$\lvert\Delta\eta\rvert > 1.15$	0.063	10.39	1.24
	$900\,\text{GeV} < m_{tt} < 1100\,\text{GeV}$	0.020	–	0.005
1500	2 fat jets ($p_T > 350\,\text{GeV}$, $R < 1.5$)	4.05	46390.00	91.50
	2 top-tagged jets	0.24	9.24	5.98
	$\lvert\Delta\eta\rvert > 1.3$	0.06	0.41	0.094
	$1350\,\text{GeV} < m_{tt} < 1550\,\text{GeV}$	0.04	–	0.009

Table 1. Cut flow table for two values of KK Higgs mass.

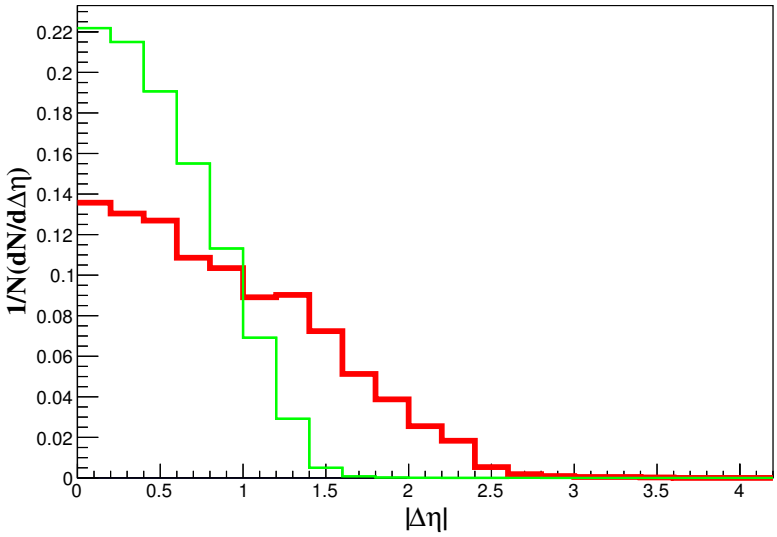

Figure 6. Normalised distribution of the absolute value of $\Delta\eta$ of two top-tagged jets. The red distribution represents signal for a h_1 mass of 1.5 TeV and green represents $t\bar{t}$ background.

invariant mass lies within a window about the h_1 mass. The distribution of the invariant mass of the pair of top-tagged jets (m_{tt}) for the signal and $t\bar{t}$ background is plotted in figure 7. Due to the effect of final state radiation (FSR), the peak of the invariant mass gets smeared mostly in the lower region of m_{tt}, as can be seen in figure 7. The cut flow table for two benchmark points are given in table 1.

Since the number of background events are comparable to the number of signal events, we calculated the significance[6] using [54],

$$\sigma = \sqrt{2\,(S+B)\ln\left(1+\frac{S}{B}\right) - 2S}\,, \tag{3.1}$$

where S is the number of signal events and B is the number of background events.

[6]When $S/B \gg 1$, it coincides with our usual $S/\sqrt{B}$.

JHEP11(2016)075

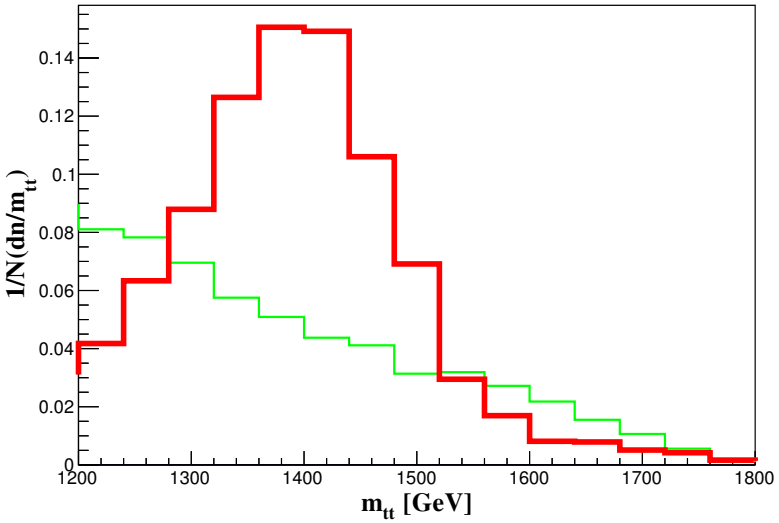

Figure 7. Normalised distribution of the invariant mass of top-tagged jet pair. The red distribution represents signal for a h_1 mass of 1.5 TeV and green represents $t\bar{t}$ background.

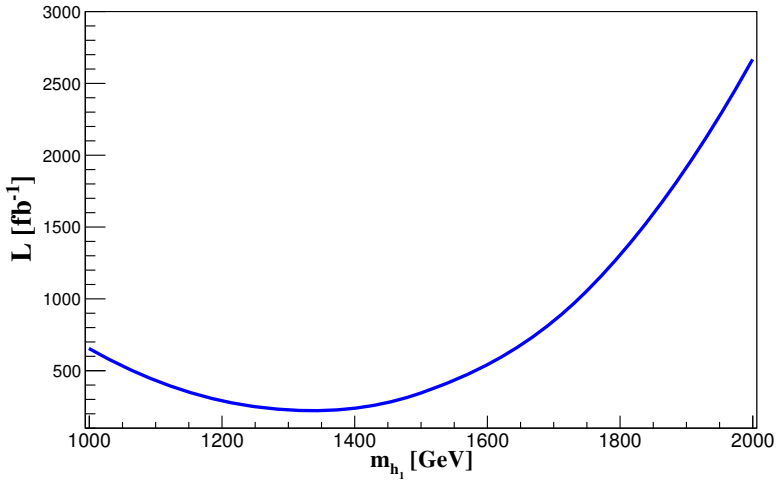

Figure 8. Luminosity required to probe the KK Higgs as a function of its mass.

The discovery reach for the h_1 of 1 TeV is about 650 fb^{-1} luminosity for $\sqrt{s}$ = 14 TeV. As the mass of the KK Higgs increases, the dijet as well as $t\bar{t}$ backgrounds fall rapidly and one can probe it with even lower luminosity. In figure 8, we plotted the luminosity required to discover the KK Higgs with 5σ discovery. In the range of 1 TeV, due to large SM backgrounds, we applied stronger cuts which reduces the signal. Thus, we need more than 600 fb^{-1} of integrated luminosity to discover it. Once the mass increases, the SM background falls and it is possible to observe the KK Higgs having a mass around 1.2 TeV with about 200 fb^{-1} of integrated luminosity at $\sqrt{s}$ = 13 TeV. Beyond 1.8 TeV, the production cross section decreases severely due to s-channel suppression and thus, we need about 1000 fb^{-1} of integrated luminosity.

JHEP11(2016)075

4 Conclusion

In order to address the gauge hierarchy problem, it is sufficient to have Higgs close to the IR brane ($b \geq 2$) and not necessarily brane localised. We find that with $b = 2$, which is the best fit value consistent with the electroweak analysis, one can have h_1 much lighter than the first KK mode of gauge bosons. The orthogonality relations among the KK profiles prevent the coupling of the h_1 to the massive gauge bosons at the tree level. We observe that the branching ratio of h_1 decaying to a pair of SM Higgs is about 1%. Thus, the h_1 decays dominantly to a pair of $t\bar{t}$.

We have focussed on the $t\bar{t}$ decay mode of h_1 where both the tops are decaying hadronically. Such a h_1 is produced at the LHC via gluon-gluon fusion. The reducible background for this topology is the SM dijet background and the irreducible background is the SM $t\bar{t}$ background. We find that using the substructure of the boosted top, especially tagging the fat jets using HEPTopTagger, QCD background reduces drastically. We find that by applying cuts on the kinematic variable such as transverse momentum (p_T) and absolute value of the rapidity difference ($\Delta\eta$) of the tagged-top jets, we could suppress the irreducible background as well. In fact, one can discover a h_1 having a mass lying in the range of 1.1–1.6 TeV at 13 TeV center of mass energy with an integrated luminosity of about $300\,\text{fb}^{-1}$. The high luminosity LHC on the other hand will be able to probe the full range between 1 and 2 TeV.

To conclude, we have shown that it is possible to explore the first KK mode of Higgs hitherto considered beyond the reach of LHC.

Acknowledgments

We would like to thank Abhishek Iyer for discussion and for collaboration at the early stages of this work. KS was visiting CRAL, IPNL Lyon and CERN Theory Department while this work was carried out and would like to gratefully acknowledge their hospitality.

A 5-dimensional Higgs action

The action in eq. (2.1) can be expressed as

$$
\begin{aligned}
S = \int d^4x dy \Bigg(& \left(-\frac{1}{2} e^{-2ky} H \partial_\mu \partial^\mu H(x,y) - e^{-4ky} a k^2 \frac{H(x,y)^2}{2} - \frac{H(x,y)}{2} \partial_y (e^{-4ky} \partial^y H(x,y)) \right) \\
& + \left(\frac{1}{2} \partial_y (H e^{-4ky} \partial_y H) - \frac{\partial^2 \lambda^1}{\partial H^2}_{|H=v} \frac{H^2}{2} e^{-4ky} \delta(y - R\pi) + \frac{\partial^2 \lambda^0}{\partial H^2}_{|H=v} e^{-4ky} \frac{H^2}{2} \delta(y) \right) \\
& + \left(\frac{1}{2} \partial_y (v e^{-4ky} \partial^y v) - \lambda^1 e^{-4ky} \delta(y - R\pi) + \lambda^0 \delta(y) \right) \\
& + \left(\partial_y (H e^{-4ky} \partial^y v) - \frac{\partial \lambda^1}{\partial H}_{|H=v} H e^{-4ky} \delta(y - R\pi) + \frac{\partial \lambda^0}{\partial H}_{|H=v} H e^{-4ky} \delta(y) \right) \\
& + \left(\frac{-v}{2} \partial_y (e^{-4ky} \partial^y v) - \frac{e^{-4ky}}{2} a k^2 v^2 \right) + H(-\partial_y (e^{-4ky} \partial^y v) - a k^2 e^{-4ky} v) \Bigg) + S_{\text{int}} \,, \qquad \text{(A.1)}
\end{aligned}
$$

where the covariant derivative is

$$D_M = \partial_M - ig_W T^a W_M^a - ig_B Y B_M \,,$$

and

$$\begin{aligned} S_{\rm int} = \int d^4x dy \sqrt{-g} \Big(& Hv(g_W^2 W_M^+ W^{M-} + g_W^2 W_M^3 W^{M3} + g_B^2 B_M B^M - 2g_B g_W B_M W^{M3}) \\ & + \frac{v^2}{4}(g_W^2 W_M^+ W^{M-} + g_W^2 W_M^3 W^{M3} + 2g_B^2 B_M B^M - 4g_B g_W B_M W^{M3}) \\ & + \frac{H^2}{4}(g_W^2 W_M^+ W^{M-} + g_W^2 W_M^3 W^{M3} + 2g_B^2 B_M B^M - 4g_B g_W B_M W^{M3}) \Big) \\ & - \left(\frac{\partial^3 \lambda^1}{\partial H^3}_{|H=v} \frac{H^3}{6} + \frac{\partial^4 \lambda^1}{\partial H^4}_{|H=v} \frac{H^4}{24} \right) \delta(y - R\pi) + L_{\rm yuk} \Big) \,. \end{aligned} \tag{A.2}$$

The equation of motion for the profiles of the vev ($v(y)$) and $h^n(x)$ can be deduced from the expansion of the action in eq. (A.1). The tadpole term of H vanishes using equation of motion of $v(y)$.

The masses of the gauge bosons are given by $M_W = g_W v_{\rm SM}/2$, $M_Z = M_W/\cos\theta_w$ and $M_\gamma = 0$ where $\cos\theta_w = g_W/\sqrt{g_W^2 + g_B^2}$.

References

[1] L. Randall and R. Sundrum, *A large mass hierarchy from a small extra dimension*, *Phys. Rev. Lett.* **83** (1999) 3370 [hep-ph/9905221] [INSPIRE].

[2] T. Gherghetta, *A Holographic View of Beyond the Standard Model Physics*, in *Physics of the Large and the Small, Proceedings of the Theoretical Advanced Study Institute in Elementary Particle Physics (TASI 2009)*, C. Csaki and S. Dodelson eds., Workd Scientific (2010), [arXiv:1008.2570] [INSPIRE].

[3] S. Raychaudhuri and K. Sridhar, *Particle Physics of Brane Worlds and Extra Dimensions*, Cambridge University Press (2016).

[4] A. Pomarol, *Gauge bosons in a five-dimensional theory with localized gravity*, *Phys. Lett.* **B 486** (2000) 153 [hep-ph/9911294] [INSPIRE].

[5] T. Gherghetta and A. Pomarol, *Bulk fields and supersymmetry in a slice of AdS*, *Nucl. Phys.* **B 586** (2000) 141 [hep-ph/0003129] [INSPIRE].

[6] Y. Grossman and M. Neubert, *Neutrino masses and mixings in nonfactorizable geometry*, *Phys. Lett.* **B 474** (2000) 361 [hep-ph/9912408] [INSPIRE].

[7] S.J. Huber and Q. Shafi, *Fermion masses, mixings and proton decay in a Randall-Sundrum model*, *Phys. Lett.* **B 498** (2001) 256 [hep-ph/0010195] [INSPIRE].

[8] G. Burdman, *Flavor violation in warped extra dimensions and CP asymmetries in B decays*, *Phys. Lett.* **B 590** (2004) 86 [hep-ph/0310144] [INSPIRE].

JHEP11(2016)075

[9] S.J. Huber, *Flavor violation and warped geometry*, *Nucl. Phys.* **B 666** (2003) 269 [hep-ph/0303183] [INSPIRE].

[10] S. Casagrande, F. Goertz, U. Haisch, M. Neubert and T. Pfoh, *Flavor Physics in the Randall-Sundrum Model: I. Theoretical Setup and Electroweak Precision Tests*, *JHEP* **10** (2008) 094 [arXiv:0807.4937] [INSPIRE].

[11] M. Bauer, S. Casagrande, U. Haisch and M. Neubert, *Flavor Physics in the Randall-Sundrum Model: II. Tree-Level Weak-Interaction Processes*, *JHEP* **09** (2010) 017 [arXiv:0912.1625] [INSPIRE].

[12] K. Agashe, G. Perez and A. Soni, *Flavor structure of warped extra dimension models*, *Phys. Rev.* **D 71** (2005) 016002 [hep-ph/0408134] [INSPIRE].

[13] M. Quirós, *Higgs Bosons in Extra Dimensions*, *Mod. Phys. Lett.* **A 30** (2015) 1540012 [arXiv:1311.2824] [INSPIRE].

[14] C. Csáki, J. Erlich and J. Terning, *The effective Lagrangian in the Randall-Sundrum model and electroweak physics*, *Phys. Rev.* **D 66** (2002) 064021 [hep-ph/0203034] [INSPIRE].

[15] G. Burdman, *Constraints on the bulk standard model in the Randall-Sundrum scenario*, *Phys. Rev.* **D 66** (2002) 076003 [hep-ph/0205329] [INSPIRE].

[16] J.L. Hewett, F.J. Petriello and T.G. Rizzo, *Precision measurements and fermion geography in the Randall-Sundrum model revisited*, *JHEP* **09** (2002) 030 [hep-ph/0203091] [INSPIRE].

[17] K. Agashe, A. Delgado, M.J. May and R. Sundrum, *RS1, custodial isospin and precision tests*, *JHEP* **08** (2003) 050 [hep-ph/0308036] [INSPIRE].

[18] K. Agashe, R. Contino, L. Da Rold and A. Pomarol, *A custodial symmetry for $Zb\bar{b}$*, *Phys. Lett.* **B 641** (2006) 62 [hep-ph/0605341] [INSPIRE].

[19] H. Davoudiasl, S. Gopalakrishna, E. Ponton and J. Santiago, *Warped 5-Dimensional Models: Phenomenological Status and Experimental Prospects*, *New J. Phys.* **12** (2010) 075011 [arXiv:0908.1968] [INSPIRE].

[20] A.M. Iyer, K. Sridhar and S.K. Vempati, *Bulk Randall-Sundrum models, electroweak precision tests and the 125 GeV Higgs*, *Phys. Rev.* **D 93** (2016) 075008 [arXiv:1502.06206] [INSPIRE].

[21] J.A. Cabrer, G. von Gersdorff and M. Quirós, *Warped Electroweak Breaking Without Custodial Symmetry*, *Phys. Lett.* **B 697** (2011) 208 [arXiv:1011.2205] [INSPIRE].

[22] J.A. Cabrer, G. von Gersdorff and M. Quirós, *Suppressing Electroweak Precision Observables in 5D Warped Models*, *JHEP* **05** (2011) 083 [arXiv:1103.1388] [INSPIRE].

[23] M. Carena, A. Delgado, E. Ponton, T.M.P. Tait and C.E.M. Wagner, *Precision electroweak data and unification of couplings in warped extra dimensions*, *Phys. Rev.* **D 68** (2003) 035010 [hep-ph/0305188] [INSPIRE].

[24] K. Agashe, A. Belyaev, T. Krupovnickas, G. Perez and J. Virzi, *LHC Signals from Warped Extra Dimensions*, *Phys. Rev.* **D 77** (2008) 015003 [hep-ph/0612015] [INSPIRE].

[25] B. Lillie, L. Randall and L.-T. Wang, *The bulk RS KK-gluon at the LHC*, *JHEP* **09** (2007) 074 [hep-ph/0701166] [INSPIRE].

[26] M. Guchait, F. Mahmoudi and K. Sridhar, *Associated production of a Kaluza-Klein excitation of a gluon with a $t\bar{t}$ pair at the LHC*, *Phys. Lett.* **B 666** (2008) 347 [arXiv:0710.2234] [INSPIRE].

JHEP11(2016)075

[27] B.C. Allanach, F. Mahmoudi, J.P. Skittrall and K. Sridhar, *Gluon-initiated production of a Kaluza-Klein gluon in a Bulk Randall-Sundrum model*, *JHEP* **03** (2010) 014 [arXiv:0910.1350] [INSPIRE].

[28] K. Agashe et al., *LHC Signals for Warped Electroweak Neutral Gauge Bosons*, *Phys. Rev.* **D 76** (2007) 115015 [arXiv:0709.0007] [INSPIRE].

[29] K. Agashe, S. Gopalakrishna, T. Han, G.-Y. Huang and A. Soni, *LHC Signals for Warped Electroweak Charged Gauge Bosons*, *Phys. Rev.* **D 80** (2009) 075007 [arXiv:0810.1497] [INSPIRE].

[30] A.M. Iyer, F. Mahmoudi, N. Manglani and K. Sridhar, *Kaluza-Klein gluon + jets associated production at the Large Hadron Collider*, *Phys. Lett.* **B 759** (2016) 342 [arXiv:1601.02033] [INSPIRE].

[31] F. Ledroit, G. Moreau and J. Morel, *Probing RS scenarios of flavour at LHC via leptonic channels*, *JHEP* **09** (2007) 071 [hep-ph/0703262] [INSPIRE].

[32] A. Djouadi, G. Moreau and R.K. Singh, *Kaluza-Klein excitations of gauge bosons at the LHC*, *Nucl. Phys.* **B 797** (2008) 1 [arXiv:0706.4191] [INSPIRE].

[33] K. Agashe and G. Servant, *Warped unification, proton stability and dark matter*, *Phys. Rev. Lett.* **93** (2004) 231805 [hep-ph/0403143] [INSPIRE].

[34] H. Davoudiasl, T.G. Rizzo and A. Soni, *On direct verification of warped hierarchy-and-flavor models*, *Phys. Rev.* **D 77** (2008) 036001 [arXiv:0710.2078] [INSPIRE].

[35] H. Davoudiasl, B. Lillie and T.G. Rizzo, *Off-the-wall Higgs in the universal Randall-Sundrum model*, *JHEP* **08** (2006) 042 [hep-ph/0508279] [INSPIRE].

[36] G. Cacciapaglia, C. Csáki, G. Marandella and J. Terning, *The Gaugephobic Higgs*, *JHEP* **02** (2007) 036 [hep-ph/0611358] [INSPIRE].

[37] S. Gopalakrishna, T. Mandal, S. Mitra and G. Moreau, *LHC Signatures of Warped-space Vectorlike Quarks*, *JHEP* **08** (2014) 079 [arXiv:1306.2656] [INSPIRE].

[38] M. Frank, N. Pourtolami and M. Toharia, *Bulk Higgs and the 750 GeV diphoton signal*, arXiv:1607.04534 [INSPIRE].

[39] P.R. Archer, M. Carena, A. Carmona and M. Neubert, *Higgs Production and Decay in Models of a Warped Extra Dimension with a Bulk Higgs*, *JHEP* **01** (2015) 060 [arXiv:1408.5406] [INSPIRE].

[40] ATLAS, CMS collaborations, *Combined Measurement of the Higgs Boson Mass in pp Collisions at $\sqrt{s} = 7$ and 8 TeV with the ATLAS and CMS Experiments*, *Phys. Rev. Lett.* **114** (2015) 191803 [arXiv:1503.07589] [INSPIRE].

[41] ATLAS collaboration, *Measurements of the Higgs boson production and decay rates and coupling strengths using pp collision data at $\sqrt{s} = 7$ and 8 TeV in the ATLAS experiment*, *Eur. Phys. J.* **C 76** (2016) 6 [arXiv:1507.04548] [INSPIRE].

[42] CMS collaboration, *Combination of standard model Higgs boson searches and measurements of the properties of the new boson with a mass near 125 GeV*, CMS-PAS-HIG-13-005.

[43] P. Cox, A.D. Medina, T.S. Ray and A. Spray, *Radion/Dilaton-Higgs Mixing Phenomenology in Light of the LHC*, *JHEP* **02** (2014) 032 [arXiv:1311.3663] [INSPIRE].

[44] ATLAS collaboration, *Measurement of the $t\bar{t}$ production cross-section using $e\mu$ events with b-tagged jets in pp collisions at $\sqrt{s} = 13$ TeV with the ATLAS detector*, *Phys. Lett.* **B 761** (2016) 136 [arXiv:1606.02699] [INSPIRE].

JHEP11(2016)075

[45] CMS collaboration, *Measurement of the top quark pair production cross section in proton-proton collisions at* $\sqrt{s} = 13$ *TeV*, *Phys. Rev. Lett.* **116** (2016) 052002 [arXiv:1510.05302] [INSPIRE].

[46] A. Alloul, N.D. Christensen, C. Degrande, C. Duhr and B. Fuks, *FeynRules 2.0 — A complete toolbox for tree-level phenomenology*, *Comput. Phys. Commun.* **185** (2014) 2250 [arXiv:1310.1921] [INSPIRE].

[47] J. Alwall et al., *The automated computation of tree-level and next-to-leading order differential cross sections and their matching to parton shower simulations*, *JHEP* **07** (2014) 079 [arXiv:1405.0301] [INSPIRE].

[48] R.D. Ball et al., *Parton distributions with LHC data*, *Nucl. Phys.* **B 867** (2013) 244 [arXiv:1207.1303] [INSPIRE].

[49] T. Plehn and M. Spannowsky, *Top Tagging*, *J. Phys.* **G 39** (2012) 083001 [arXiv:1112.4441] [INSPIRE].

[50] G. Kasieczka, T. Plehn, T. Schell, T. Strebler and G.P. Salam, *Resonance Searches with an Updated Top Tagger*, *JHEP* **06** (2015) 203 [arXiv:1503.05921] [INSPIRE].

[51] T. Sjöstrand, S. Mrenna and P.Z. Skands, *A Brief Introduction to PYTHIA 8.1*, *Comput. Phys. Commun.* **178** (2008) 852 [arXiv:0710.3820] [INSPIRE].

[52] Y.L. Dokshitzer, G.D. Leder, S. Moretti and B.R. Webber, *Better jet clustering algorithms*, *JHEP* **08** (1997) 001 [hep-ph/9707323] [INSPIRE].

[53] S. Bentvelsen and I. Meyer, *The Cambridge jet algorithm: Features and applications*, *Eur. Phys. J.* **C 4** (1998) 623 [hep-ph/9803322] [INSPIRE].

[54] G. Cowan, K. Cranmer, E. Gross and O. Vitells, *Asymptotic formulae for likelihood-based tests of new physics*, *Eur. Phys. J.* **C 71** (2011) 1554 [*Erratum ibid.* **C 73** (2013) 2501] [arXiv:1007.1727] [INSPIRE].

JHEP11(2016)075